

A fast, low cost, and highly efficient fluorescent DNA labeling method using methyl green

Daniel Prieto · Gonzalo Aparicio · Pablo E. Morande · Flavio R. Zolessi

Accepted: 14 March 2014
© Springer-Verlag Berlin Heidelberg 2014

Abstract The increasing need for multiple-labeling of cells and whole organisms for fluorescence microscopy has led to the development of hundreds of fluorophores that either directly recognize target molecules or organelles, or are attached to antibodies or other molecular probes. DNA labeling is essential to study nuclear-chromosomal structure, as well as for gel staining, but also as a usual counterstain in immunofluorescence, FISH or cytometry. However, there are currently few reliable red to far-red-emitting DNA stains that can be used. We describe herein an extremely simple, inexpensive and robust method for DNA labeling of cells and electrophoretic gels using the very well-known histological stain methyl green (MG). MG used in very low concentrations at physiological pH proved to have relatively narrow excitation and emission spectra, with peaks at 633 and 677 nm, respectively, and a very high resistance to photobleaching. It can be used in combination with other common DNA stains or antibodies without any visible interference or bleed-through. In electrophoretic gels, MG also labeled DNA in a similar way to ethidium bromide, but, as expected, it did not label RNA. Moreover, we show here that MG fluorescence can be used as a stain for direct measuring of viability by both microscopy and flow

cytometry, with full correlation to ethidium bromide staining. MG is thus a very convenient alternative to currently used red-emitting DNA stains.

Keywords Methyl green · DNA · Flow cytometry · Confocal microscopy · Electrophoresis · Fluorescence

Introduction

Microscopy imaging has been a pillar of biological research since the invention of the first microscopes, and in the post-genomic era, it has clearly become an essential tool for the further advancement in the full molecular characterization of cells and organisms. Fluorescence microscopy, and in particular laser scanning confocal microscopy (LSCM), is routinely used for most molecular studies on biological processes. This has been aided by the relatively recent development of multiple fluorophores specially designed for laser excitation and long-lasting fluorescence emission (Panchuk-Voloshina et al. 1999; Terai and Nagano 2013). Many of these compounds are, however, relatively expensive.

Fluorescent DNA staining is widely used for routine counterstaining of tissues and cells, as well as for the detailed study of nuclear and chromosomal structure for research and clinical diagnosis (Klonisch et al. 2010). Although several DNA stains are currently available, traditionally, the most widely used have been those excited by UV light and emitting in blue, like DAPI or Hoechst minor groove-binding agents (Kapuscinski 1995; Latt and Stetten 1976). The reason for this is that these fluorophores fit in the usual three-filter systems used in most conventional epifluorescence microscopes, being typically combined with green and orange-red-emitting fluorophores that can

Electronic supplementary material The online version of this article (doi:10.1007/s00418-014-1215-0) contains supplementary material, which is available to authorized users.

D. Prieto · G. Aparicio · F. R. Zolessi (✉)
Sección Biología Celular, Facultad de Ciencias, Universidad de la República, Uruguay, Iguá 4225, 11400 Montevideo, Uruguay
e-mail: fzolessi@fcien.edu.uy

D. Prieto · P. E. Morande · F. R. Zolessi
Institut Pasteur de Montevideo, Matajojo 2020,
11400 Montevideo, Uruguay

be easily attached to antibodies or other molecules (like FITC and TRITC, respectively). The progressive incorporation of spectral detection in LSCMs, combined with a wide variety of laser emission lines, has allowed researchers to choose for the use of far-red-emitting nuclear stains such as propidium iodide (PI) or TO-PRO 3 (Van Hooijdonk et al. 1994). In addition, UV lasers are relatively expensive, and it is rather common for institutions to have LSCMs not equipped for blue fluorophore detection. Another problem faced by microscopists is that many cells and tissues, particularly in embryos, contain autofluorescence emitting in a wide range of wavelengths, from blue to orange. Far-red fluorophores have helped to overcome this problem (Beumer et al. 1995).

Methyl green (MG) is a triphenylmethane dye which has been widely used as a nuclear colored stain for histological sections since the late 19th century (Høyer et al. 1986) and for biochemical analysis of DNA degradation (De Petrocellis and Parisi 1973; Kurnick and Sandeen 1960). It binds to DNA, but not RNA, in a non-intercalating manner, interacting with the major groove and showing preferential binding for AT-rich regions (Kim and Nordén 1993; Krey and Hahn 1975; Kurnick 1952; Kurnick and Foster 1950). Although its field of application has been mostly restricted to bright field microscopy, some reports suggest its use in fluorescent staining protocols for microscopy as a quencher of DNA fluorescence (Li et al. 2003). As MG was shown not to bind RNA, it has also been used as a complement for RNA determination by Pironin Y in flow cytometry, because it blocks the non-specific binding of this dye to DNA (Pollack et al. 1982).

In a search for a rapid and stable nuclear staining for confocal microscopy in the red/far-red region of the visible spectrum, we found that an extremely diluted aqueous MG solution at physiological pH provided a suitable and extremely convenient alternative to currently used fluorophores. In this article, we describe applications for this dye in fluorometry, confocal microscopy, gel electrophoresis and flow cytometry, along with an initial characterization of its relevant physico-chemical properties.

Materials and methods

Methyl green solution preparation

We used a 2 % MG stock solution obtained by chloroform extraction to remove crystal violet impurities, according to classical methods (Kurnick and Foster 1950). Briefly, an aqueous 4 % MG (Dr. G. Grübler, Leipzig, Germany) solution was separated several times with chloroform until no traces of violet stain could be seen, either using a separation funnel and discarding the lower phase (chloroform) or

a test tube and carefully recovering the upper phase (aqueous solution).

In vitro fluorometric assays

125 ng/mL and 10 µg/mL MG solutions (1:16,000 and 1:2,000 from 2 % stock, respectively) with or without 100 µg/mL calf thymus DNA were prepared in phosphate-buffered saline (PBS). UV-visible spectra were performed with a Varian Cary 50 UV-VIS spectrophotometer (Agilent Technologies, Santa Clara, CA, USA). Quantitation of fluorescent emission was determined with a Cary Eclipse fluorescence spectrophotometer (Agilent Technologies, Santa Clara, CA, USA) under a fixed excitation wavelength of 633 nm recording emission from 645 to 800 nm. The data interval was set to 1 nm; the emission slit was set to 10 nm; and the detection scan was performed at 120 nm/min. Maximal dilutions were used whenever possible in order to avoid internal filter effects.

Embryo staining procedure for in situ observation

For in toto staining, zebrafish embryos were fixed at the desired stage with 4 % paraformaldehyde in PBS, overnight at 4 °C. After washing in PBS-T (1 % Triton X-100), embryos were incubated for 3 h at room temperature to overnight at 4 °C with gentle agitation with the fluorophores diluted in PBS-T as follows: 2–4 µg/mL MG (1:10,000 to 1:5,000 from 2 % stock); 0.1–0.2 µg/mL propidium iodide (1:10,000 to 1:5,000 from 1 mg/mL stock), 1 µM TO-PRO-3 (1:1,000 from 1 mM stock) or 0.1–0.2 µg/mL Hoechst 33342 (1:10,000 to 1:5,000 from 1 mg/mL stock). Indirect immunofluorescence was performed according to standard procedures, and MG or Hoechst 33342 counterstaining was achieved by mixing with the secondary antibodies solution and incubating overnight at 4 °C. Cryosections from paraformaldehyde-fixed, gelatin-embedded chick embryos were processed for immunofluorescence as described (Zolessi and Arruti 2001) and counterstained with MG and/or Hoechst 33342 by a final incubation of 5–15 min at room temperature. Cultured cells (not shown) were treated in a similar way. Both whole embryos and tissue sections were mounted in 70 % glycerol in PBS, pH 7.4. Microscopic observation and image acquisition of MG-stained tissues were done using a spectral detection LSCM, Leica TCS-SP5 (Leica Microsystems GmbH Wetzlar, Germany), equipped with five lasers (LED 405 nm, Argon multiple-line 458–514 nm; HeNe 543 nm; HeNe 594 nm; HeNe 633 nm), 20× water-glycerol-oil immersion (NA 0.70), 63× oil immersion (NA 1.4), and 63× water immersion (NA 1.2) objectives. It has a resonant scanner at 800 Hz, with a maximal resolution of 1,024 × 1,024 pixels. Images

were processed using open source software: FIJI-ImageJ 1.47n (Schindelin et al. 2012) and GIMP 2.6 (GNU Image Manipulation Program).

In situ quantitation of fluorescent DNA staining

Quantitative assessment of MG, propidium iodide and TO-PRO-3 fluorescence in situ was performed using whole-mounted zebrafish embryos, only stained for each of these fluorophores. Simple optical sections of selected embryonic regions (usually neural retina or brain because of their high nuclear density) were obtained under different conditions. Measurements were made during image acquisition using the LAS AF software version 2.6.0.7266 (Leica Microsystems GmbH Wetzlar, Germany) by marking an elliptical or rectangular ROI (region of interest), depending on the shape and size of the observed tissue. In all cases, we used a 63× water immersion objective (1.2 NA), simple scans (no averaging or accumulation), the pinhole set at Airy 1, a $1,024 \times 1,024$ scanning field and a scanner zoom of 1.7×.

For registering the whole emission spectrum, the $xy\lambda$ scanning mode was used, with a detection window of 5 nm and a 3 nm step, spanning a wide range in the visible spectrum. Emission intensity at different laser excitation lines was determined by performing short spectra ($xy\lambda$) of 4–7 points around the region of maximal emission for each fluorophore (propidium iodide, 640–655 nm; TOPRO-3, 651–662 nm; MG, 664–682 nm), and picking the maximum value in each measurement. Photobleaching was assessed either by a continuous xyt acquisition or by quantitating the spectrum peak ($xy\lambda$) at different times during continuous excitation with laser for up to 30 min. Laser line used was 633 nm for MG and TO-PRO-3 and 488 nm for propidium iodide, in most cases at 30 % power (except when noted in figure or text).

MG staining of DNA for agarose gels

Methyl green was incorporated as a 1:5,000–1:10,000 dilution of the stock into a 1 % agarose gel matrix in TAE. Ethidium bromide was incorporated at 0.5 $\mu\text{g}/\text{mL}$. MG and ethidium bromide gels were loaded with DNA (Mass-Ruler sm0403 from Thermo Fisher Scientific, Waltham, for quantitative purposes, or 100 bp DNA ladder from Life Technologies, Carlsbad, for comparative gels) or RNA (0.5–10 kb RNA ladder, Invitrogen) molecular weight ladders at different concentrations and electrophoresed at the same time using standard methods. Images of the electrophoresed nucleic acids were obtained with a G:Box (Syngene, Frederick, USA) either under epi-illumination with red light (635 nm) and a 705 M band-pass filter, with a 30–60 s exposure, or with a standard mid-wave UV transillumination.

Cell viability assays

For microscopic assessment of viability, human peripheral blood mononuclear cells (PBMCs) from healthy donors were thawed from liquid N_2 , incubated for 30 min in RPMI supplemented with 10 % FBS and immediately prior to confocal imaging were incubated with 0.1 volume of a mixture of 100 $\mu\text{g}/\text{mL}$ acridine orange, 100 $\mu\text{g}/\text{mL}$ ethidium bromide and 4 $\mu\text{g}/\text{mL}$ MG. For flow cytometric determination of cell viability, human Raji (B cell Burkitt's lymphoma) cells (5×10^5) purchased at ATCC (Manassas, USA) were cultured in HEPES-buffered RPMI 1640 medium supplemented with 10 % fetal calf serum, 50 $\mu\text{g}/\text{mL}$ gentamicin, and 2 mM L-glutamine at 37 °C in a humidified CO_2 atmosphere in absence or presence of Fludarabine (9- β -D-arabinosyl-2-fluoroadenine-monophosphate) obtained from Sigma-Aldrich used at 50 or 100 $\mu\text{g}/\text{mL}$ (Gandhi and Plunkett 2002). After 24 h of incubation, cells were labeled using 10 $\mu\text{g}/\text{mL}$ propidium iodide and 4 $\mu\text{g}/\text{mL}$ MG and immediately acquired in a CyAn Flow Cytometer (Beckman Coulter, Indianapolis, USA). Data were analyzed using Summit v4.3 software from Dako Inc., USA. Markers were settled according to the fluorescent signals detected in unstained cells, using the same acquisition parameters as in labeled cells.

Results

MG absorption and emission profiles in solution

To initially characterize MG fluorescence properties, we performed a light absorption spectrum of MG in a spectrophotometric assay, and determined it had three absorption maxima at 244, 377 and 633 nm (Fig. 1a). Adding DNA to the solution did not alter this absorption profile.

Excitation of MG through excitation at these three wavelengths in the absence of DNA resulted in an emission peak at 488 nm when an excitation beam of 244 nm was used, and a smaller peak with an emission maximum at 750 nm, when a 377 nm light was used. No fluorescence emission was detected when exciting MG in solution at 633 nm (Fig. 1b).

We further analyzed the 633 nm absorption maximum by comparing the fluorometric emission profile of MG alone and in the presence of DNA (Fig. 1c). Surprisingly, an important emission peak appeared at the range of 663–686 nm when DNA was added, with a maximum that is around 7.5 times higher than the corresponding curve range in the absence of DNA. This peak showed a sustained decrease, reaching background levels just after 800 nm, and indicated that MG fluorescence properties dramatically change after binding to DNA.

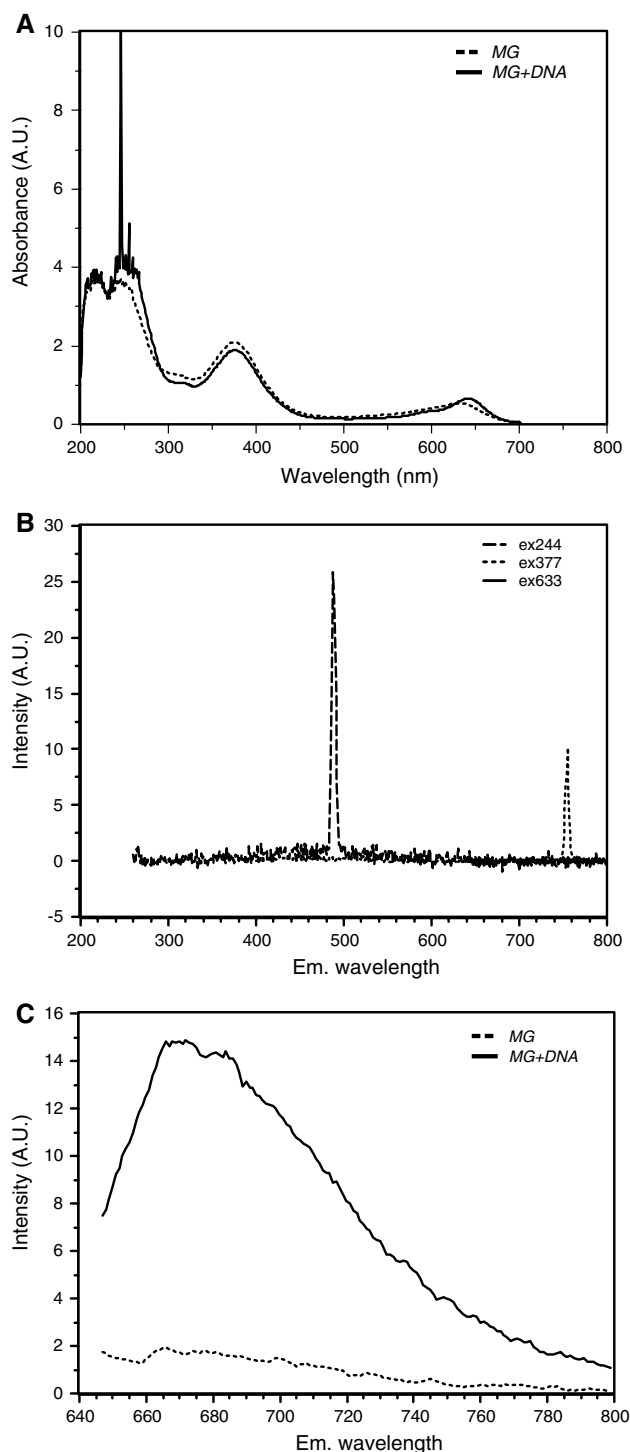


Fig. 1 Spectral properties of methyl green in solution. **a** Absorption spectra of MG (10 µg/mL), both free and in the presence of DNA, displayed maxima at 244, 377 and 633 nm. In the presence of DNA, the DNA 280 nm absorption peak was added, plus a protein contamination peak at 260 nm. **b** Fluorescent emission of free MG (125 ng/mL) when 244, 377 and 633 nm excitation wavelengths were applied. Excitation at 244 nm elicited an emission peak at 488 nm; excitation at 377 nm elicited an emission peak at 750 nm; excitation at 633 nm elicited no detectable emission peaks. **c** Excitation of MG (10 µg/mL) at 633 nm results in an emission peak with a maximum at 650 nm in the presence of DNA

MG fluorescence upon nuclear staining: excitation and emission

To further characterize DNA-bound MG fluorescence, we used it at diluted aqueous solutions, unable to cause visible color staining, to label nuclei on fixed tissues. Using whole-mounted zebrafish embryos stained with MG, we assessed the ideal excitation conditions for spectral detection confocal microscopy, using laser lines 458, 476, 488, 496, 514, 543, 594 and 633 nm. As expected, maximal fluorescence intensity for MG at the DNA-specific range was achieved at $\lambda = 633$ nm (Fig. 2a); hence, this is the excitation wavelength we used in subsequent microscopy experiments. With the other laser excitation lines, MG far-red fluorescent signal was very close to background. Remarkably, TO-PRO-3 gave a nearly identical excitation curve, also with a maximum at 633 nm, while propidium iodide showed a wider range of excitation, with two maximal peaks at 488 and 514 nm and signal significantly above background between 476 and 543 nm (Fig. 2a).

Using the spectral quantitative mode in the LSCM (LAS AF acquisition software), we also measured the emission spectra of these three red/far-red-emitting fluorophores. Similar to what was seen in solution, maximal signal for MG was achieved at 677 nm, rather far from the excitation wavelength at 633 nm, while for TO-PRO-3, it was relatively closer, at 649 nm (Fig. 2b). Propidium iodide fluorescence emission was measured by exciting at its 488 nm peak to give a cleaner spectrum, and in these conditions, maximal signal was at 609 nm (Fig. 2b). As the emission spectra were clearly different in shape, we compared sharpness of the peaks by measuring their width at 50 % of the maximal intensity. TO-PRO-3 gave the sharpest spectrum, with a 50 % emission band of 35 nm (636–671 nm), followed by MG with 67 nm (649–716 nm) and propidium iodide with 87 nm (584–671 nm) (Fig. 2b).

MG fluorescence upon nuclear staining: photobleaching

Photobleaching is another usual inconvenient of many fluorophores, particularly when high resolution confocal images of thick specimens are desired, requiring long exposure times. We assessed sensitivity of MG and the other fluorophores to photobleaching by continuous excitation with the appropriate laser at 30 % power. While in these conditions, TO-PRO-3 signal decayed to undetectable in less than 2 min when exciting with the 633 nm laser, MG signal remained extremely stable for a very long time, with a loss of around only 1 % in 30 min (Fig. 2c). Using a 100 % percent laser power gave very similar results for MG photobleaching (not shown). Propidium iodide also proved to be rather stable when excited at 488 nm (albeit much less

Fig. 2 Quantitative assessment of methyl green properties as a fluorophore for laser excitation microscopy. **a** Comparative fluorescence response of MG, TO-PRO-3 and propidium iodide (PI), measured at the maximum emission peak for each fluorophore, upon the excitation with different laser lines with a spectral detection laser scanning confocal microscope. **b** Emission intensity spectra of propidium iodide (PI), TO-PRO-3 and MG, exciting with their respective ideal laser lines, as determined in a. **c** Temporal profile of fluorescence emission decay for propidium iodide (PI), TO-PRO-3 and MG after continuous excitation with their ideal laser lines (30 % power). The *inset* shows a comparison of the fluorescence emission decay only for TO-PRO-3 and MG after a prolonged time of continuous excitation (30 min), measuring at 5 min intervals

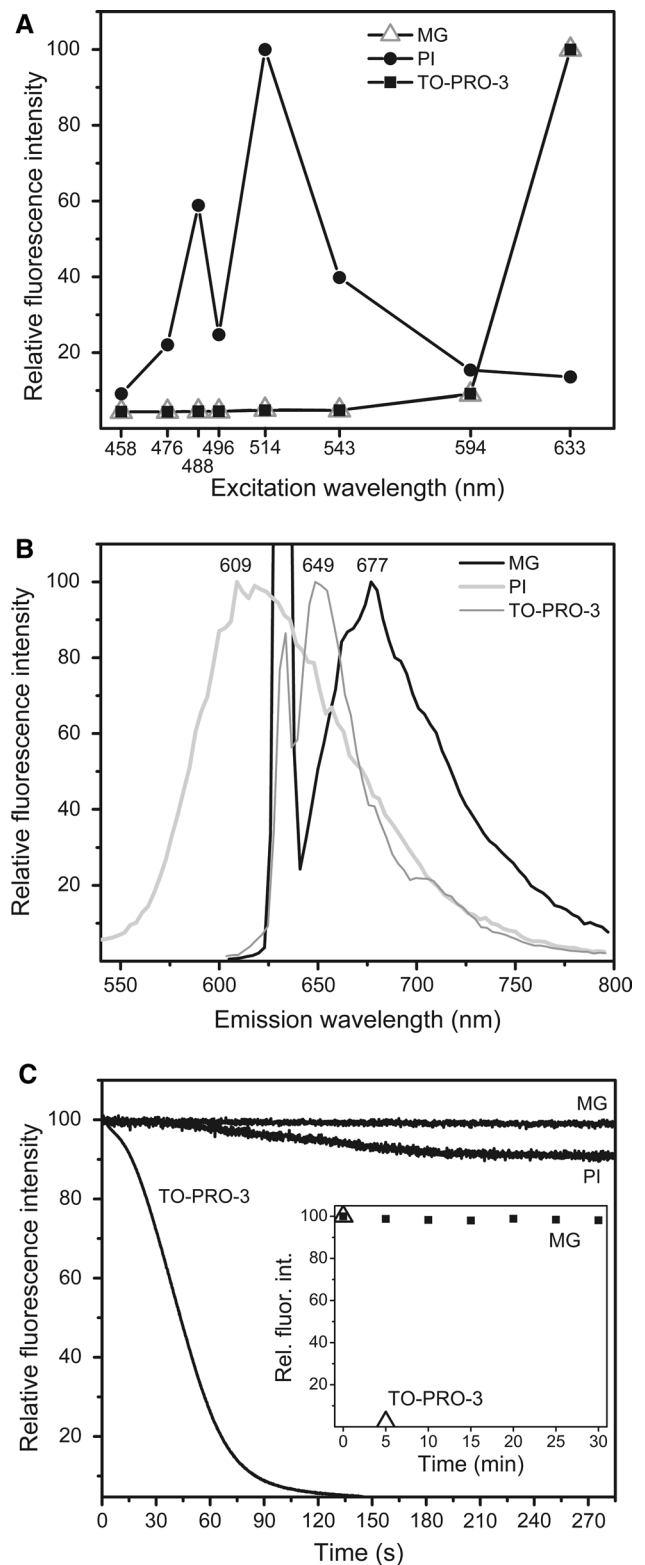
than MG), losing around 10 % of its fluorescence signal in 4–5 min (Fig. 2c).

MG as an ideal fluorescent nuclear stain for embryonic tissues

We assayed MG ability to be used as a nuclear stain for whole-mounted and sectioned embryonic tissues, using zebrafish whole embryos and chick embryo cryosections (Fig. 3). Remarkably, whole body staining of zebrafish embryos was achieved within 3 h of incubation. Confocal sections of the zebrafish retina and olfactory pit, as well as chick neural plate region, revealed staining of DNA with very good sub-nuclear resolution (Fig. 3). This label was stable, and it did not interfere with other fluorophores, antibodies or phalloidin actin labeling (Fig. 3). Furthermore, we did not find interference with other DNA stains such as Hoechst 33342, a minor groove-interacting molecule. Figure 4 shows two series of images taken from chick embryo cryosections at neurula stage, doubly labeled with Hoechst 33342 and MG. When tissues were massively irradiated for zoomed images using the 63× water immersion objective (1.2 NA), MG labeling did not exhibit a noticeable decay in fluorescence emission, as expected, allowing us to acquire 0.2 μm spaced z-stacks for 3D reconstruction in both, zebrafish whole embryos and chick embryo sections (see an example in Online Resource 1).

MG as a staining procedure specific for DNA in agarose gels

As MG can fluorescently label DNA in vitro, we examined its suitability for staining electrophoresed DNA in agarose gels. We analyzed the ability of MG to stain different amounts of DNA fragments of different sizes using a quantitated commercial DNA ladder (Fig. 5a). Interestingly, MG proved to be able to allow for the detection of at least 4.8 ng of a 1.5 kb DNA fragment (Fig. 5a, lane 2, arrowhead) under red (635 nm) epi-illumination. As the most commonly used stain for DNA in gels is ethidium bromide, we also decided to compare MG with this stain



for the labeling of electrophoresed DNA and RNA. Separate gels with either stain were identically loaded with samples of commercial DNA and RNA ladder. Interestingly, while ethidium bromide labeled, as it is well known, both

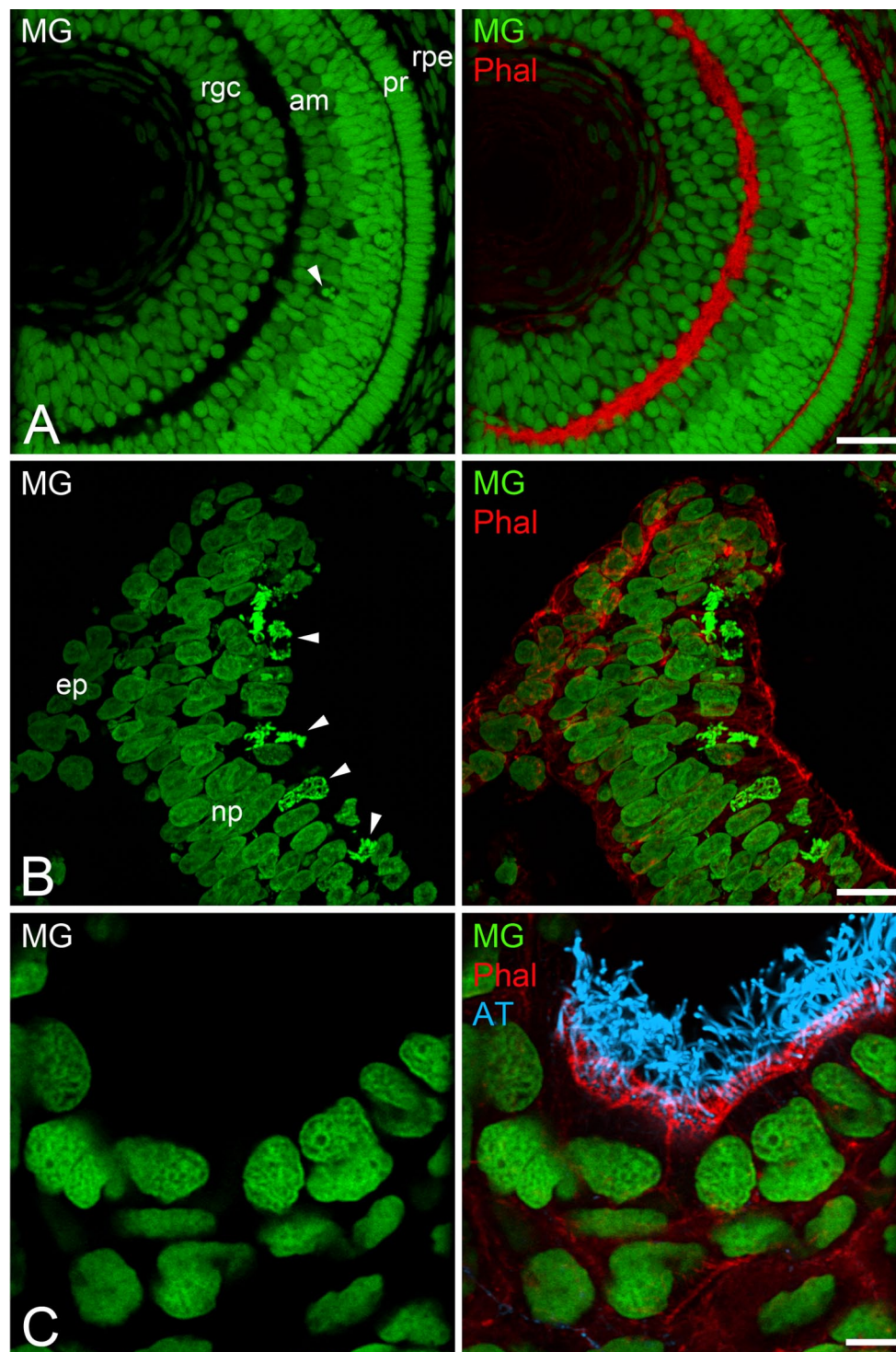


Fig. 3 Examples of embryonic tissues stained with methyl green and different fluorescent markers. **a** Confocal section through the retina of a whole-mounted 60 hpf zebrafish embryo labeled with MG and TRITC-conjugated Phalloidin to highlight regions enriched in actin filaments. MG clearly demarcates all nuclei and even allows for the identification of different cell types based on nuclear size and shape, as well as chromatin condensation. The arrowhead points to a pyknotic nucleus. *am* amacrine cells in the inner nuclear layer, *pr* photoreceptors, *rgc* retinal ganglion cells, *rpe* retinal pigmentary epithelium. **b** Maximum intensity projection of 10 confocal slices obtained from

a chick embryo cryosection, labeled with MG and TRITC-Phalloidin. The *image* shows the region of the neural plate-epidermal border. Several mitotic cells are clearly evidenced by the very strong MG labeling of their chromosomes (*arrowheads*). *ep* presumptive epidermis, *np* neural plate. **c** Maximum intensity projection of 3 confocal slices from a whole-mounted 48 hpf zebrafish embryo labeled with MG, TRITC-Phalloidin and an antibody to acetylated tubulin (highlighting cilia). The high magnification image shows the olfactory pit, where MG very clearly labels subnuclear chromatin structure. *Scale bars*: a–b, 20 μm ; c, 5 μm

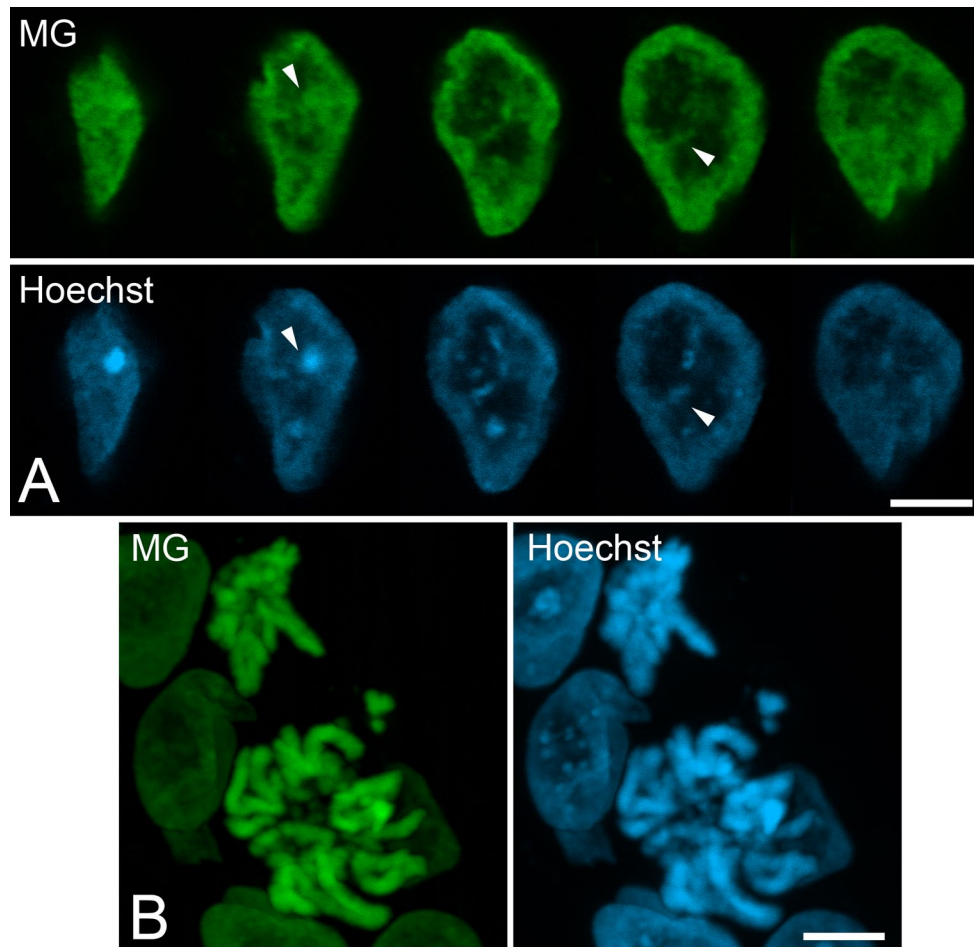


Fig. 4 High magnification confocal sections of chick embryonic tissue double-labeled with MG and Hoechst 33342. **a** Series of selected optical sections through a nucleus from an ectodermal cell of a neurula-stage chick embryo cryosection. Comparison of MG and Hoechst staining of the same nuclei, showing nuclear and sub-nuclear structure. The *arrowheads* point to condensed chromatin structures

highlighted by both compounds, but with different relative levels of intensity. **b** Maximum intensity projection of a confocal stack from a chick neurula cryosection, showing interphasic and mitotic endodermal cells. Mitotic chromosome morphology is revealed at very similar resolution and staining pattern for both compounds. See a 3D reconstruction in Online Resource 1. *Scale bars: 5 μ m*

nucleic acids with similar intensities, MG was only able to efficiently detect DNA (Fig. 5b). An extremely weak RNA label could be detected, indicating that even if MG might be able to show some RNA binding, its affinity for RNA must be several times lower than that for DNA.

MG as a cell viability stain in fresh and cultured cells

To assess the ability of MG to act as a vital stain, we labeled live human PBMCs from healthy donors and found it to stain only a small fraction of the cells (not shown). This observation made us wonder if viable cells could be actively excluding MG, and if labeled cells could actually be dead or dying. Some DNA intercalating molecules, such as propidium iodide and ethidium bromide show this property, and are hence very commonly used to assess cell viability. When comparing MG with ethidium bromide on

these living cells, we found a 1:1 correlation on the number of labeled cells (Fig. 6a), indicating that MG can also be used to assess cell viability. In contrast, the cell permeant intercalating stain acridine orange labeled the full cell population under the same conditions (Fig. 6a).

Finally, we evaluated the performance of MG as a direct measure of cell viability by flow cytometry. We chose to work with Raji cells, a lymphoblastic-like B line of human origin. As shown in the upper charts of Fig. 6b, forward versus size gating of viable or dead cells (R1 or R2) correlated with low and high percentage of positive cells, respectively, for both MG and the well-known viability stain propidium iodide. This shows a correlation in the percentages of cell death and cell viability between forward versus size cytometric analysis and MG positive and negative stain, respectively. In addition, when treated with the cytotoxic purine analog Fludarabine, commonly used in

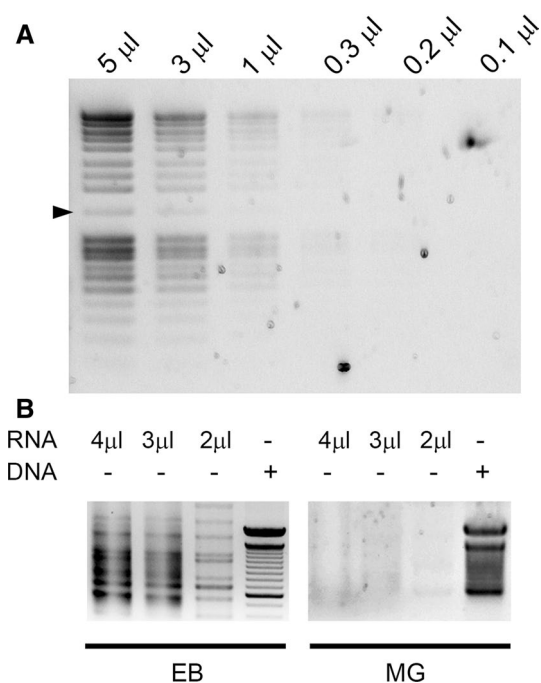


Fig. 5 Methyl green as an efficient and specific fluorescent stain for DNA gel electrophoresis. **a** DNA in an agarose gel electrophoresis was stained with a solution of MG as described in the text. Gel lanes were loaded with the indicated volumes of DNA ladder (at 103 ng/µL). The limit of detection was determined as the 4.8 ng band of the second lane (arrowhead). **b** Comparison of DNA and RNA labeling on gels with MG and ethidium bromide. Ethidium bromide (left) and MG (right) were incorporated into agarose gels that were loaded with the indicated amounts of DNA or RNA ladder. After electrophoresis, label was evidenced using the appropriate illumination. Negative images of the fluorescence on gels are shown in **a** and **b**

cancer chemotherapy, MG stained Raji cells in identical percentages as compared to propidium iodide. As expected, this combined staining protocol resulted in double positive PI⁺MG⁺ cells, as depicted in the representative dot plots presented in the lower charts of Fig. 6b. This result confirms that MG is only able to label dead cells nuclei, in a similar manner as propidium iodide, and shows that it can be used in fluorescent-based techniques to discriminate dead or damaged cells by positive staining.

Discussion

Until now, tissue staining protocols used MG in concentrations several orders of magnitude larger than shown here (usual histological stain uses around 0.1–0.5 % solutions). Under such conditions, MG also acts as an excellent quencher of unspecific staining of nuclei and this is why it has been used as a counterstain of fluorescently labeled nucleoli (Pollack et al. 1982). It would not be surprising

that interactions of the sort described for pyronin Y by Kapuscinski and Darzynkiewicz (1987) would explain the fact that a molecule able to act as a fluorescent stain could switch its behavior to that of a quencher in a concentration-dependent manner. This fact, together with the lack of a generalized availability of spectral confocal microscopes, probably hindered MG's notable properties as a fluorescent stain. We could find only one report in the literature on the use of MG as a fluorescent DNA stain on histological preparations (Itoh et al. 2003). In this case, however, a high concentration of MG was used to generate the usual green stain visible in bright field microscopy, and the fluorescence excitation–emission wavelengths were coincident with those of orange-red fluorophores such as TRITC hence very different to the advantageous properties reported in the present work.

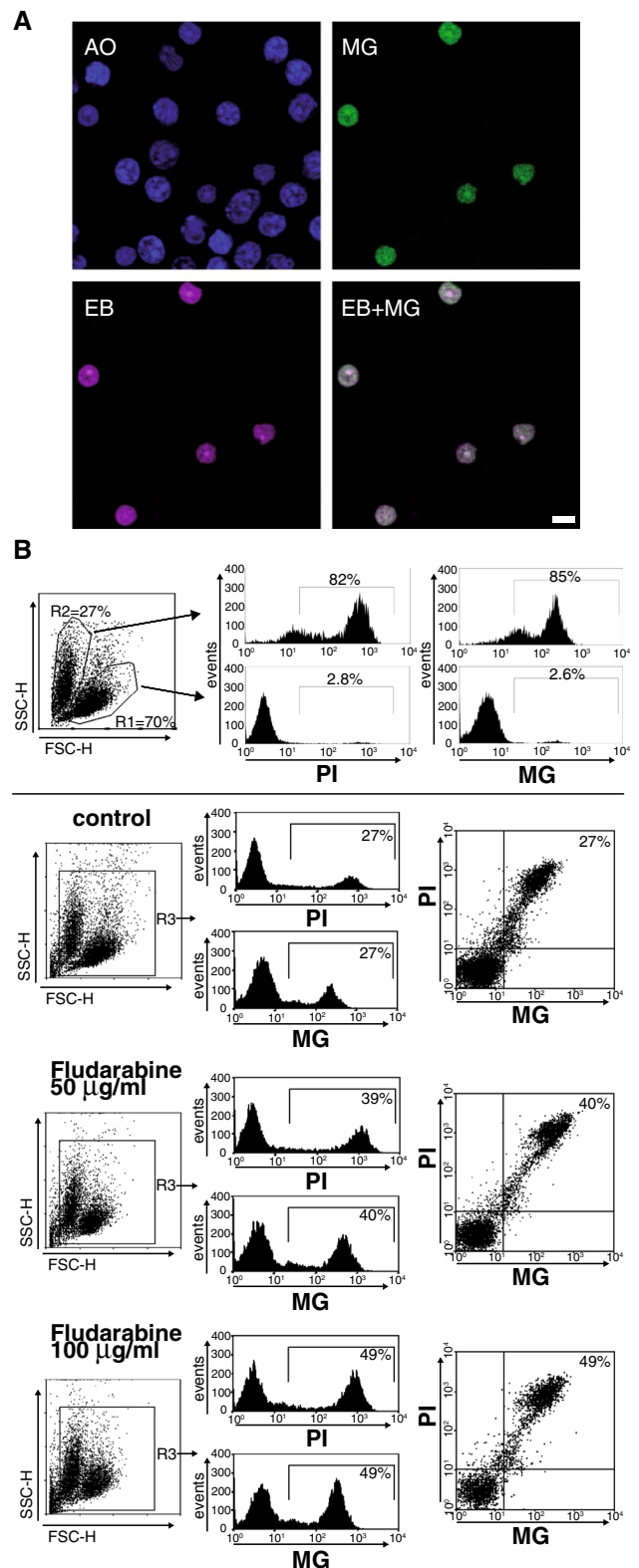
We have shown here MG's excellent qualification as a general purpose DNA staining for fluorescence microscopy with sub-nuclear resolution, and high emission levels even after being irradiated during extended periods of time. The staining procedure is extremely simple, not to mention its low cost and shelf-life stability (the stock solution is stable for months at room temperature). After its comparison with two other extensively used red fluorescent stains for nuclei, propidium iodide and TO-PRO-3, we found a much superior performance for MG. Like TO-PRO-3, MG shows a maximal excitation at 633 nm and a relatively narrow emission peak at the far-red wavelength range, while propidium iodide is excited by a wide range of shorter wavelengths, especially 488 and 514 nm, while emitting in an extremely wide range in the visible spectrum. Not only its excitation, but also its emission range, are coincident with that of several other common-use fluorophores such as FITC or TRITC (or more recently developed similar ones like the corresponding Alexas), making it a bad option for multi-color fluorescence imaging. With MG (or TO-PRO-3), however, this problem is almost inexistent as they do not or very little overlap with excitation or emission spectra of common-use blue, green or orange-red fluorophores. Indeed, MG very little overlaps with TRITC or Alexa 594, while TO-PRO-3, with an emission spectrum relatively blue-shifted, even if still little overlapping with TRITC, will have a larger overlap with Alexa 594 leading to the possibility of bleed-through. The Stokes shift is also much better for MG (44 nm) than for TO-PRO-3 (16 nm). Finally, one major problem with the very good DNA stain TO-PRO-3 is that it bleaches relatively quickly when excited, even for short periods of time. MG showed an astonishing stability of its fluorescence upon continuous excitation, even at the highest laser power. A major advantage relies in the fact that MG does not fluoresce when irradiated at 633 nm on its own, but increases several times its emission intensity when bound to DNA, making it suitable

Fig. 6 Methyl green as a cell viability stain for fluorescence microscopy and flow cytometry. **a** Confocal sections of live PBMCs stained with *AO* acridine orange, *MG* methyl green and *EB* ethidium bromide. Lower right panel shows EB/MG images overlay, evidencing complete colocalization. Scale bar: 5 μm . **b** Flow cytometric quantitation of cell viability comparing size/granularity, propidium iodide (PI) and MG staining in cultured Raji cells. Cells from the human B cell line Raji (5×10^5) were cultured in the absence or presence of Fludarabine for 24 h at the indicated concentrations. After the incubations, cells were stained for propidium iodide (PI) and methyl green (MG) labeling and immediately acquired in a flow cytometer. Shown are representative dot plots of flow cytometry analyses depicting forward versus size scattering, PI or MG histograms, or PI and MG double staining. Percentages of positive cells are indicated ($n = 3$ independent experiments). Forward versus size scattering comparative analysis of MG and PI indicates that MG only stained dead cells

for being added to mounting media as it is unnecessary to wash out the remaining MG from the samples.

These characteristics position MG as a central molecule for routine DNA staining in confocal microscopy protocols for whole embryos, as well as tissue sections or cultured cells. The recent development of different techniques that allow for the detailed observation of whole samples of tissue, such as light sheet microscopy (Amat and Keller 2013) or the CLARITY method for tissue diaphanization (Chung et al. 2013), can be greatly benefited from a very stable stain like this. The fact that both excitation and emission of MG are in the long-wavelength region of the spectrum also facilitates light penetration in both directions, with the expected generation of better quality nuclear images from thick specimens than those obtained with the more commonly used blue-emitting fluorophores (Lenz 1999). In our hands, MG did not interfere with staining with other fluorescent probes, such as small molecules, antibodies or fluorescent proteins. Regarding this, in our method MG is diluted in physiological pH buffers, with or without proteins or nonionic detergents, while the classical histological technique implies using an acetate buffer at pH 4.2, which would be incompatible with antibody co-incubation.

Furthermore, the ability of MG to stain DNA in agarose gels combined with its spectral characteristics, together with the fact that its interaction with DNA is non-intercalating but electrostatic and that its sensitivity is similar to that of ethidium bromide—not to mention its lower market value when compared to usual commercial stains—may put MG on the bench of every molecular biology lab. It is remarkable that we have assayed it under epi-illumination and found it to be a DNA stain at least as efficient as ethidium bromide in terms of detection limits. It seems probable that under strong trans-illumination conditions—such as those achieved by led arrays, it may show even better performance than we have shown here. Even if it has been classically shown that MG only labels DNA when used as



a colored stain on cells and it preferentially binds double-stranded DNA over RNA (see for example Kurnick and Foster 1950; Krey and Hahn 1975) and that there was no evident cytoplasmic signal in the fluorescent MG staining

of cells shown in the present work, we decided to confirm that MG preferentially labels DNA also as a fluorescent stain. By electrophoresis gel staining, we showed here that MG has a very strong preference for DNA above RNA labeling. This observation also makes it a potentially very useful tool to differentiate between these two nucleic acids in biological samples, for example in combination with the unspecific compound ethidium bromide.

Finally, we have demonstrated the suitability of MG to act as a reliable cell viability probe for both microscopy and flow cytometry techniques. Live peripheral PBMC labeling evaluated by fluorescence microscopy revealed that only a small fraction of cells stained for MG, a fraction which interestingly resulted to coincide with cells positive for the well-established viability staining with ethidium bromide (Kasibhatla et al. 2006). Furthermore, we evaluated MG staining by flow cytometry in fresh Raji cells and in induced cell-death experiments, using the cytotoxic purine analog Fludarabine. We found that discrimination of viable and dead cells by forward versus size scattering analysis, which represents a vastly used method for viability determination (Liegler et al. 1995), matched with negative MG staining of viable cells and positive MG staining of dead cells. Importantly, the percentages of cell death determined by MG staining were highly similar to those obtained by propidium iodide staining. Finally, Fludarabine-induced cell death showed a similar decrease in cultured cells viability, as evaluated by percentages of MG⁺ cells, percentages of PI⁺ cells, and percentages of cells obtained in forward versus size scattering analysis. Quantification of all three parameters revealed near identical results for both compounds, where dead cells were always double positive.

Altogether, data presented here show that MG can be used as a general purpose fluorescent DNA label, with excellent properties regarding excitation-emission wavelengths, fluorescence intensity and stability, product cost and shelf-life. We have also demonstrated that it can be extremely useful for multiple cell biology-related applications, and we foresee that there are many more possible, such as DNA quantitation in solution, in gels or in situ, the determination of cell cycle parameters by flow cytometry, and others. The facts that MG is an old-known compound, with a very low commercial cost, and patent-free, makes it easily accessible to any research or clinical laboratory, anywhere in the world.

Acknowledgments The authors would like to thank Dr. Cristina Arruti and Dr. Pablo Opezzo for facilitating the use of reagents and lab installations; the Cell Biology Unit at the Institute Pasteur Montevideo for access to the confocal microscope and flow cytometer; Dr. Mario Señorale for access to the G:Box. Partial funding was from Comisión Sectorial de Investigación Científica (CSIC)-Universidad de la República and PEDECIBA, Uruguay.

References

- Amat F, Keller PJ (2013) Towards comprehensive cell lineage reconstructions in complex organisms using light-sheet microscopy. *Dev Growth Differ* 55(4):563–578
- Beumer TL, Veenstra GJ, Hage WJ, Destrée OH (1995) Whole-mount immunohistochemistry on *Xenopus* embryos using far-red fluorescent dyes. *Trends Genet: TIG* 11:9
- Chung K, Wallace J, Kim S-Y, Kalyanasundaram S, Andalman AS, Davidson TJ, Mirzabekov JJ, Zalocusky KA, Mattis J, Denisin AK, Pak S, Bernstein H, Ramakrishnan C, Grosenick L, Gradinaru V, Deisseroth K (2013) Structural and molecular interrogation of intact biological systems. *Nature* 497:332–337
- De Petrocellis B, Parisi E (1973) Deoxyribonuclease in sea urchin embryos. Comparison of the activity present in developing embryos, in nuclei, and in mitochondria. *Exp Cell Res* 79:53–62
- Gandhi V, Plunkett W (2002) Cellular and clinical pharmacology of fludarabine. *Clin Pharmacokinet* 41(2):93–103
- Høyer PE, Lyon H, Jakobsen P, Andersen AP (1986) Standardized methyl green–pyronin Y procedures using pure dyes. *Histochem J* 18:90–94
- Itoh J, Umemura S, Hasegawa H, Yasuda M, Takekoshi S, Osamura YR, Watanabe K (2003) Simultaneous detection of DAB and methyl green signals on apoptotic nuclei by confocal laser scanning microscopy. *Acta Histochem Cytochem* 36:367–376
- Kapuscinski J (1995) DAPI: a DNA-specific fluorescent probe. *Bio-tech Histochem* 70:220–233
- Kapuscinski J, Darzynkiewicz Z (1987) Interactions of pyronin Y(G) with nucleic acids. *Cytometry* 8:129–137
- Kasibhatla S, Amarante-Mendes GP, Finucane D, Brunner T, Bossy-Wetzel E, Green DR (2006) Acridine orange/ethidium bromide (AO/EB) staining to detect apoptosis. *Cold Spring Harbor Protocols* 2006 (3):pdb.prot4493
- Kim SK, Nordén B (1993) Methyl green. A DNA major-groove binding drug. *FEBS Lett* 315:61–64
- Klonisch T, Wark L, Hombach-Klonisch S, Mai S (2010) Nuclear imaging in three dimensions: a unique tool in cancer research. *Ann Anat* 192:292–301
- Krey AK, Hahn FE (1975) Studies on the methyl green-DNA complex and its dissociation by drugs. *Biochemistry* 14:5061–5067
- Kurnick NB (1952) The basis for the specificity of methyl green staining. *Exp Cell Res* 3:649–651
- Kurnick NB, Foster M (1950) Methyl green. III. Reaction with deoxyribonucleic acid, stoichiometry, and behavior of the reaction product. *J Gen Physiol* 34:147–159
- Kurnick NB, Sandeen G (1960) Acid deoxyribonuclease assay by the methyl green method. *Biochim Biophys Acta* 39:226–231
- Latt SA, Stetten G (1976) Spectral studies on 33258 Hoechst and related bisbenzimidazole dyes useful for fluorescent detection of deoxyribonucleic acid synthesis. *J Histochem Cytochem* 24:24–33
- Lenz P (1999) Fluorescence measurement in thick tissue layers by linear or nonlinear long-wavelength excitation. *Appl Opt* 38(16):3662–3669
- Li B, Wu Y, Gao X-M (2003) Pyronin Y as a fluorescent stain for paraffin sections. *Histochem J* 34:299–303
- Liegler TJ, Hyun W, Yen TS, Stites DP (1995) Detection and quantification of live, apoptotic, and necrotic human peripheral lymphocytes by single-laser flow cytometry. *Clin Diagn Lab Immunol* 2(3):369–376
- Panchuk-Voloshina N, Haugland RP, Bishop-Stewart J, Bhalgat MK, Millard PJ, Mao F, Leung W-Y (1999) Alexa dyes, a series of new fluorescent dyes that yield exceptionally bright, photostable conjugates. *J Histochem Cytochem* 47:1179–1188
- Pollack A, Prudhomme DL, Greenstein DB, Irvin GL, Claffin AJ, Block NL (1982) Flow cytometric analysis of RNA content in

- different cell populations using pyronin Y and methyl green. *Cytometry* 3:28–35
- Schindelin J, Arganda-Carreras I, Frise E, Kaynig V, Longair M, Pietzsch T, Preibisch S, Rueden C, Saalfeld S, Schmid B, Tinevez J-Y, White DJ, Hartenstein V, Eliceiri K, Tomancak P, Cardona A (2012) Fiji: an open-source platform for biological-image analysis. *Nat Methods* 9:676–682
- Terai T, Nagano T (2013) Small-molecule fluorophores and fluorescent probes for bioimaging. *Pflugers Arch* 465:347–359
- Van Hooijdonk CA, Glade CP, Van Erp PE (1994) TO-PRO-3 iodide: a novel HeNe laser-excitable DNA stain as an alternative for propidium iodide in multiparameter flow cytometry. *Cytometry* 17:185–189
- Zolessi FR, Arruti C (2001) Apical accumulation of MARCKS in neural plate cells during neurulation in the chick embryo. *BMC Dev Biol* 1:7